Proceedings World Geothermal Congress 2010
Bali, Indonesia, 25-29 April 2010

Analysis of Pressure Transient Response for an Injector under Hydraulic Stimulation at the Salak Geothermal Field, Indonesia

Jorge A. Acuna

Chevron Geothermal and Power, Sentral Senayan II, 26th Floor, Jl. Asia Afrika, Jakarta 10270, Indonesia

jacuna@chevron.com

Keywords: Fall off, fractional flow, fractal flow, stimulation, Salak, Awibengkok.

ABSTRACT

Four pressure fall-off pressure transient tests were conducted in a well being stimulated by high pressure injection. The tests were analyzed with a technique based on fractional flow in a composite reservoir. The results show the progress of the stimulation process as the measured reservoir properties change from test to test. Novel techniques for analysis of pressure transient tests are demonstrated. The reason for the very large wellbore storage effect usually found in injection fall-off tests is discussed and considered in the analysis.

1. INTRODUCTION

The sequence of pressure fall-off tests (PFO's) shown in this paper have been previously analyzed by Yoshioka et al. (2009). Their analysis, however only covers the radial flow part of the tests. In this paper an alternative interpretation is made that includes the entire test. It relies on fractional flow theory.

Fractional flow behavior, and the closely related fractal flow behavior and its relevance to naturally fractured systems has been discussed by Acuna et al. (1995). In linear, radial or spherical flow the pressure derivative has the characteristic slope of 0.5, 0 and -0.5 respectively. Fractional flow allows for the derivative to have any slope in between.

A densely and uniformly fractured media in which a vertical well is completed should show typical radial flow. When many of the fractures are missing or sealed, the network has un-fractured or unconnected areas of many sizes. In this case fully developed radial flow may not be observed but rather fractional flow. Chang and Yortsos (1990) presented solutions for an infinite fractured fractal medium with and without matrix participation. Barker (1988) presented a solution very similar in the context of fractional dimension flow. The solutions without matrix participation have been explored numerically by Acuna (1993) and Palike (1998) and applied to actual cases by Acuna et al. (1995) and Leveinen (2000).

Solutions without matrix participation are suitable for fractured systems with very low matrix permeability such as geothermal reservoirs, aquifers in crystalline rock and possibly tight gas as well as shale gas reservoirs.

2. BACKGROUND

An injector well located in a geothermal field in Indonesia named Salak, also known as Awibengkok, was subjected to high pressure injection with the objective of increasing its injectivity from October 2007 to September 2008. Four pressure fall-off (PFO) tests were performed to determine the effectiveness of the stimulation. The PFO's are particularly useful because they were done while injecting in a colder low permeability area in the marginal area of the reservoir. Therefore they do not have the usual drawbacks associated to pressure transient tests in geothermal systems, namely the presence of steam or two-phases in the reservoir as well as thermal transients that take place when injecting in very hot regions.

The diagnostic pressure derivative plots of these tests show a change in the slope of the derivative at a given time. The interpretation of this behavior is that there is a change in the properties of the medium at a corresponding distance that results in different flow dimensionality. This behavior can be reproduced by a radial composite model with inner and outer areas with different properties. This case was qualitatively explored by Acuna et al. (1995) and actual pressure tests showing this behavior have been analyzed by Leveinen (2000).

The objective of this paper is to present a technique for analysis of pressure transient tests in fractional dimension composite models. It complements and extends the work of Leveinen (2000) by including expressions for drawdown based on the transition time as well as the corresponding expressions for buildup tests.

3. THEORETICAL DEVELOPMENT

The solution of Chang and Yortsos (1990) for a well in an infinite fractal medium can be written as

$$p_D(r_D,t_D) = \frac{r_D^{(2+\theta)(1-\delta)}}{\Gamma(\delta)(2+\theta)}\Gamma(\delta-1,\frac{r_D^{2+\theta}}{(2+\theta)^2 t_D}) \qquad (1)$$

Where p_D, t_D and r_D are dimensionless pressure, time and radius respectively. $\Gamma(x,y)$ is the incomplete Gamma function and $\Gamma(x)$ is the Gamma function. In Acuna et al. (1995) there is an error in this equation, the value $1-\delta$ is shown instead of $\delta-1$ in the first argument of the incomplete Gamma function, this error was also found by Palike (1998). The correct expression shown above was presented in Acuna (1993).

Fractional flow can be caused by a porous medium of variable flow area as shown by Doe (1992). In this case the connectivity is perfect and diffusion occurs normally. It can also be caused by fracture systems that cover the available space with gaps of many sizes as shown by Acuna et al. (1995). In this case diffusion is delayed as the network is not perfectly connected, the parameter θ is greater than zero and we have fractal flow. Equation 1 for fractal flow converges to the solution for fractional flow presented by Barker (1988) when θ is zero.

The parameter δ combines geometric and fluid transport properties of the fracture network. The flow dimension equals 2δ. For the case of radial flow ($\delta \rightarrow 1$, $\theta \sim 0$) the incomplete Gamma function $\Gamma(\delta-1,x)$ equals the

exponential integral function –Ei(-x), the Gamma function Γ(δ) approaches one and the familiar solution for a radial systems is obtained from Equation 1.

For long enough time, or short times at the wellbore, the following approximation derived from using the first two terms of the power series expansion of the incomplete Gamma function can be used.

$$p_D(r_D,t_D)=\frac{(2+\theta)^{1-2\delta}}{\Gamma(\delta)}\frac{t_D^{1-\delta}}{(1-\delta)}-\frac{r_D^{(2+\theta)(1-\delta)}}{(1-\delta)(2+\theta)} \qquad (2)$$

3.1 Drawdown analysis

When dealing with a composite medium the time of change in derivative slope is called the transition time τ. For times less than then transition time τ the system behaves as an infinite medium with the characteristics of the inner medium. Therefore drawdown for $t < \tau$ is given by

$$p_D(t_D)=\frac{(2+\theta)^{1-2\delta}}{\Gamma(\delta)}\frac{t_D^{1-\delta}}{1-\delta}-\frac{1}{(1-\delta)(2+\theta)}+S \qquad (3)$$

Where p_D is dimensionless pressure for the inner region or region 1 and t_D is dimensionless time.

For times larger than the transition time ($t \geq \tau$), the presence of the inner region can be accounted for as a pseudo-skin. The expression for the drawdown equation for $t \geq \tau$ in terms of the contact radius ρ_D is as follows

$$p_D(t_D)=\left(\frac{(2+\theta)^{1-2\delta}}{\Gamma(\delta)}\frac{t_D^{1-\delta}}{1-\delta}-\frac{\rho_D^{(2+\theta)(1-\delta)}}{(1-\delta)(2+\theta)}\right)_2$$

$$+\left(\frac{\rho_D^{(2+\theta)(1-\delta)}-1}{(1-\delta)(2+\theta)}+S\right)_1\frac{P_1^*}{P_2^*} \qquad (4)$$

Where subscripts 1 and 2 on the lower right side of the parenthesis mean that properties inside correspond to those regions. P_i^* is the ratio between actual pressure and dimensionless pressure for region i.

Equation 4 can also be expressed in terms of the transition time τ as follows

$$p_D(t_D)=\left(\frac{(2+\theta)^{1-2\delta}}{\Gamma(\delta)}\frac{t_D^{1-\delta}-\tau_D^{1-\delta}}{1-\delta}\right)_2$$

$$+\left(\frac{(2+\theta)^{1-2\delta}}{\Gamma(\delta)}\frac{\tau_D^{1-\delta}}{1-\delta}-\frac{1}{(1-\delta)(2+\theta)}+S\right)_1\frac{P_1^*}{P_2^*} \qquad (5)$$

By inspection of the two expressions it follows that the distance to the interface between the two regions ρ_D can be calculated by equating the pseudo-skin. The expression valid for the two regions is

$$\rho_D=\frac{(2+\theta)^{\frac{2}{2+\theta}}}{\Gamma(\delta)^{\frac{1}{(2+\theta)(1-\delta)}}}\tau_D^{\frac{1}{2+\theta}} \qquad (6)$$

Equation 6 can be interpreted as a radius of investigation.

3.2 Buildup analysis

Buildup equations can be obtained from the drawdown equations and again there are two expressions, one for times before the time of change in derivative slope Δτ and another for afterward.

For $\Delta t \leq \Delta\tau$ the expression is the following

$$p_D(t_D)=\left(\frac{(2+\theta)^{1-2\delta}}{\Gamma(\delta)}\frac{(t_{pD}+\Delta t_D)^{1-\delta}-\Delta\tau_D^{1-\delta}}{1-\delta}\right)_2\frac{P_2^*}{P_1^*}$$

$$+\left(\frac{(2+\theta)^{1-2\delta}}{\Gamma(\delta)}\frac{\Delta\tau_D^{1-\delta}-\Delta t_D^{1-\delta}}{1-\delta}\right)_1 \qquad (7)$$

As before subscripts 1 and 2 on the lower right side of the parenthesis mean that properties inside correspond to those regions.

For times $\Delta t > \Delta\tau$ the analysis shows that region 2 can be analyzed as if it were an infinite medium with characteristics equal to region 2. The equation is

$$p_D(t_D)=\frac{(2+\theta)^{1-2\delta}}{\Gamma(\delta)}\frac{(t_{pD}+\Delta t_D)^{1-\delta}-\Delta t_D^{1-\delta}}{1-\delta} \qquad (8)$$

The distance to the interface is obtained from Equation 6.

For the case of buildups the technique to solve the problem starts by solving the outer region first. The fractional flow time is defined as $T_f=\frac{(t_p+\Delta t)^{1-\delta}-\Delta t^{1-\delta}}{1-\delta}$ and the derivative dP/dT_f is calculated. A graph of pressure and pressure derivative versus T_f will show a horizontal pressure derivative plot when the correct value of δ is selected.

The slope *m* of the pressure versus T_f graph is given by.

$$m=\frac{(2+\theta)^{(1-2\delta)}}{\Gamma(\delta)}\frac{P}{T_*^{1-\delta}} \qquad (9)$$

P* and T* represent the ratio of dimensional to dimensionless pressure and time respectively defined as $P^*=\frac{q\mu\, r_w^{\theta}}{(CF_P)2\pi(kh)_0}$ and $T^*=\frac{\mu\, r_w^{2+\theta}}{CF_T}\left(\frac{\Phi ch}{kh}\right)_0$. CF_P and CF_T are conversion factors for pressure and time; CF_P is 1 for consistent units and $1.127*10^{-3}$ for oil and gas customary units. CF_T equals 1 for consistent units and $2.637*10^{-4}$ for oil and gas customary units with time in hours. The flow rate *q* is volumetric flow rate at reservoir conditions (qB_o in oil and gas customary units). The subscript "$_0$" next to *kh* and Φ*ch* mean that these values are only valid at $r_D = 1$.

In radial flow as $\delta \rightarrow 1$ T_f converges to $\ln\left(\frac{t_p+\Delta t}{\Delta t}\right)$, Γ(x) approaches 1 and the plot becomes a common Horner plot with Equation 9 used to estimate *kh* directly. Contrary to the case of radial flow, however the slope of the fractional flow graph contains also information about Φ*ch* and *kh* may not be calculated directly.

4. EXAMPLE OF ANALYSIS

The diagnostic plot of the first PFO tests is shown in Figure 1. There is a dimensionality transition that occurs at a time close to 20 hours. The early part of the test seems to behave as typical radial flow.

The second part of the test is fractional flow with a derivative slope close to 0.35. The composite fractional

flow model is a very appealing model in our case because this well has been stimulated with water injection at a temperature 200F less than the rock. Injection pressure is above the fracture closure pressure. The injectivity has increased with time and it is expected that by the time this test was performed a region close to the wellbore has been fractured by thermal shock as well as pressure.

The analysis technique presented here is applicable even to the first part of the test as radial flow is just a special case of fractional flow.

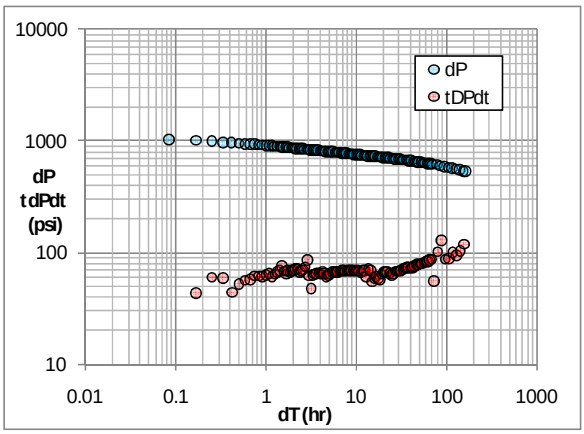

Figure 1. Diagnostic plot of first fall-off test showing a dimensional transition characterized by the change in slope in the derivative curve.

The first step in analyzing the buildup test is to evaluate the late part that is unaffected by the presence of the inner region. Rewriting Equation 7 in dimensional form and using Equation 9 we have

$$\Delta p(\Delta t) = mT_f = m\frac{(t_p + \Delta t)^{1-\delta} - \Delta t^{1-\delta}}{1-\delta} \qquad (10)$$

Calculating *Tf* as well as dP/dT_f and iterating on δ until the derivative is flat we get Figure 2. The pressure difference is calculated with respect to a final pressure such that the difference becomes zero when *Tf* equals 0.

From the slope and using Equation 9 we get $\frac{P_*}{T_*^{1-\delta}} = 39.03\cdot$

As presented in Chang and Yortsos (1990) fluid flow properties change with distance from the well as $k(r) = k_0 r_D^{(2+\theta)(\delta-1)}$ and $\Phi(r) = \Phi_0 r_D^{2(\delta-1)}$. The value of θ cannot be determined without additional information, however it is not expected to be large. An assumption of θ ~ 0 will be made in this paper. Le Borgne et al. (2004) shows how multi-well tests can be used to obtain a value for θ.

In a fractured medium it is expected that the change in permeability and porosity with distance from the well is due to a change in the number and connectivity of fractures transporting fluid. To keep the analysis parallel to conventional pressure transient derivations it is assumed that the embedding geometry is cylindrical.

For the analysis of the early part of the test we reformulate Equation 7 in dimensional form as follows

$$\Delta p(t) - m_2\frac{(t_p + \Delta t)^{1-\delta_2} - \Delta\tau^{1-\delta_2}}{1-\delta_2} = m_1\frac{\Delta\tau^{1-\delta_1} - \Delta t^{1-\delta_1}}{1-\delta_1} \qquad (11)$$

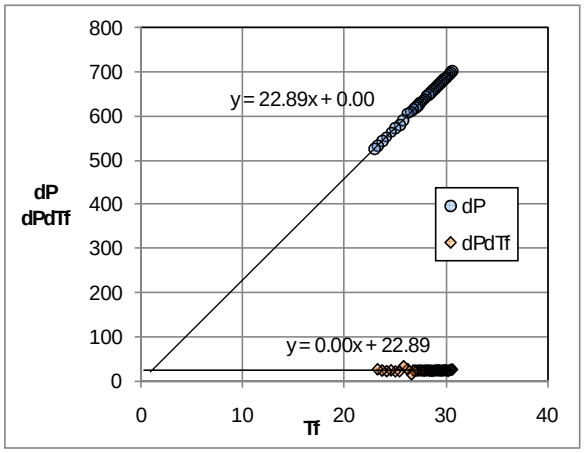

Figure 2. Fractional flow plot for the later part of the PFO shown in Figure 1 for a selection of δ = 0.653. Only data after the transition time Δτ = 28 hrs are shown. Best fitting lines are shown.

All values in the left hand side are known after solving for the late time part of the test. Thus we calculate the left hand side and plot versus T_f as defined in the right hand side. Δτ is the transition time equals 28 hours. Figure 3 shows the resulting fractional flow plot for the early part of the test.

In this well where injection has taken place for weeks and near wellbore fracturing is present it is safe to assume that there is no skin factor. Any near wellbore improvement will be captured by the inner region characterization.

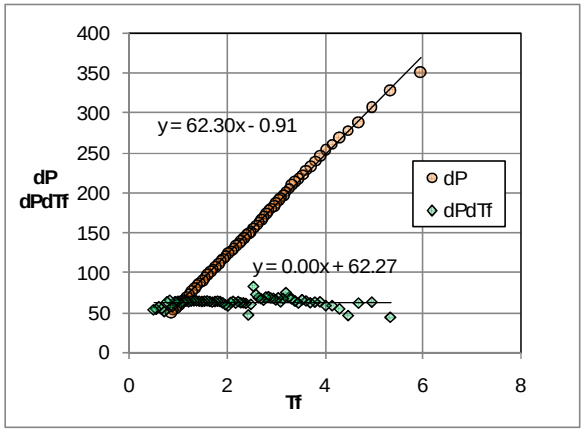

Figure 3. Fractional flow plot for the early part of the PFO shown in Figure 1 showing the fit for a selection of δ = 0.952. Only data before the transition time Δτ = 28 hrs are shown.

With this assumption the drawdown Equation 5 and the buildup Equation 7 are subtracted and used to estimate P* for region 1. In dimensional form this equation valid for Δt ≤ Δτ is

$$\frac{1}{(1-\delta_1)(2+\theta_1)}P_1^* = \Delta p(t) - m_2\frac{(t_p + \Delta t)^{1-\delta_2} - t_p^{1-\delta_2}}{1-\delta_2}$$

$$+ m_1\frac{\Delta t^{1-\delta_1}}{1-\delta_1} \qquad (12)$$

ΔP is (p_{wf} - p_{si}) for buildup and (p_{si} - p_{wf}) for fall-off tests. The second term to the right is negligible when $t_p >> \Delta t$. We get P^*_1 = 103.95 and with Equation 9 we get T^*_1 = 0.049.

To solve the radius of contact between the two regions we use Equation 6 with the known value of T* for region 1 to obtain ρ_D = 35.22. Since the wellbore radius equals 0.51 ft we have a radius of contact of 18 ft.

The values of T* for region 2 can be obtained by using Equation 6 again with the value of ρ_D just found. In this case we obtain T^*_2 = 0.036 and from Equation 9 we get P^*_2 = 12.30. Once P* and T* are calculated values of *kh* and φch are obtained and shown in Table 1.

5. RESULTS AND DISCUSSION

Figure 4 shows the pressure and pressure derivative match for the 4 PFO's analyzed. Very early time deviations can be due to using Equation 2 as an approximation to Equation 1. It is also apparent that there is no wellbore storage period. This could be due to the earliest data being recorded 5 minutes after shut-in.

The derivative shape of test 3 and 4 suggest that more that 2 regions may be needed to improve the match. The technique shown here can be easily extended to more than 2 regions.

Table 1 presents the parameters calculated for the four PFO's. The tests show an increasing permeability in the two regions from test to test. Additionally the asymptotic pressure (Pinf) keeps decreasing which may be showing a better connection to the main geothermal reservoir that is at a much lower pressure that this marginal region.

Test	Tp	Pinf	δ_1	$kh_0 1$	$\Phi ch_0 1$	δ_2	$kh_0 2$	$\Phi ch_0 2$	Interface
	days	psi		mD-ft	ft/psi		mD-ft	ft/psi	ft
PFO 1	74	1966	0.95	7979	2.58	0.65	67452	16.0	17.9
PFO 2	84	1842	0.95	8746	2.65	0.61	97997	20.8	17.4
PFO 3	112	1876	0.90	15077	2.07	0.62	135895	13.8	25.4
PFO 4	207	1753	0.85	30670	0.99	0.64	201585	5.2	51.1

Table 1. Tp is the effective time injecting at 24 bpm (64 l/s). Pinf is the pressure at which the test converges at very long times. Φch includes fracture dilation effects.

The value of the fractional flow parameter δ in both regions is remarkably consistent. The inner region (Region 1) is not only increasing in permeability but also in size. The distance to the interface with the outer region (Region 2) increases from test to test.

Figure 5 (top) shows the permeability thickness product kh versus radial distance. Despite large values of *kh* shown in Table 1 for the maximum value for Region 2 kh is never larger than 10000 mD-ft. Assuming a thickness of 3000 ft which should be typical of a geothermal reservoir this represents a permeability of less than 4 mD at the interface between the two regions. This shows how the restriction to flow occurs in the outer region as should be expected in a permeability stimulation process.

The φch values obtained are remarkably high. Figure 5 (bottom) shows the variation with distance from the well. Using the same typical reservoir thickness and a typical porosity the resulting compressibility is a few orders of magnitude too high compared to that of water at 350 F.

Injection at pressure above fracture closure pressure as occurred in these tests, results in fracture dilation. The associated compressibility of a dilated system is that of the entire system as the fracture volume changes with pressure. As discussed by Van den Hoek (2002), when analyzed conventionally this results in a wellbore storage coefficient that is orders of magnitude too high. In reality the effect of wellbore storage itself is negligible in comparison to the dilation effect of the fracture system. This effect is known as fracture compliance. Fracture compliance can still be interpreted as a product of fracture volume and total compressibility including fracture dilation effects, therefore the notation will be kept as φch. Fracture compliance is treated in the equations as a large wellbore storage coefficient. By using using $\frac{t_D}{C_D}$ instead of t_D it is observed that values of φch obtained in these tests should be interpreted as $\frac{C}{2\pi r_w^2}$ where C is the fracture compliance in ft^3/psi. As the fracture volume changes with radius it is intuitively expected that the volume of reservoir subject to dilation also changes with radius, but the explanation of the variation of fracture compliance with radius is beyond the scope of this paper.

Fracture compliance decreases in later tests signaling that the relative volume change of the pore space with pressure is less. This should be consistent with more fractures remaining open and the observed increased permeability.

The values of φch, actually $\frac{C}{2\pi r_w^2}$, in Figure 5 (bottom) result in a maximum fracture compliance value of 4.2 ft^3/psi (0.95 bbl/psi) comparable to values reported in the literature. The wellbore storage is less than 1% of the fracture compliance value.

The variation of permeability-thickness with radius we have adopted in this discussion is just a convenient assumption. In reality what we interpret as a change in *kh* could be due to a change in flow area in a medium with constant permeability as shown by Doe (1991), or as a variation of the permeability area product as described by Barker (1988) and Leveinen (2000).

In naturally fractured reservoirs such as Awibengkok we expect that the permeability of the individual fractures can change dramatically from fracture to fracture. Over large areas, however the combined effect of fractures produces a bulk permeability that can be effectively measured with multi and single well tests. The concept of fracture permeability as a bulk property distributed over large areas is consistent with the approach taken here.

Work with numerical models of fractured networks (Acuna, 1993) show that there is direct correlation between pressure derivative slope changes and fracture network property known as the radial mass even at very small distances. Radial mass is just the volume of fractures as it changes with distance from the well.

The radial variation of properties at short distances from the well may be unique to a well position but as the pressure pulse expands away from the well and engages more fractures. Other wells should have similar late time responses as they engage larger reservoir area with time.

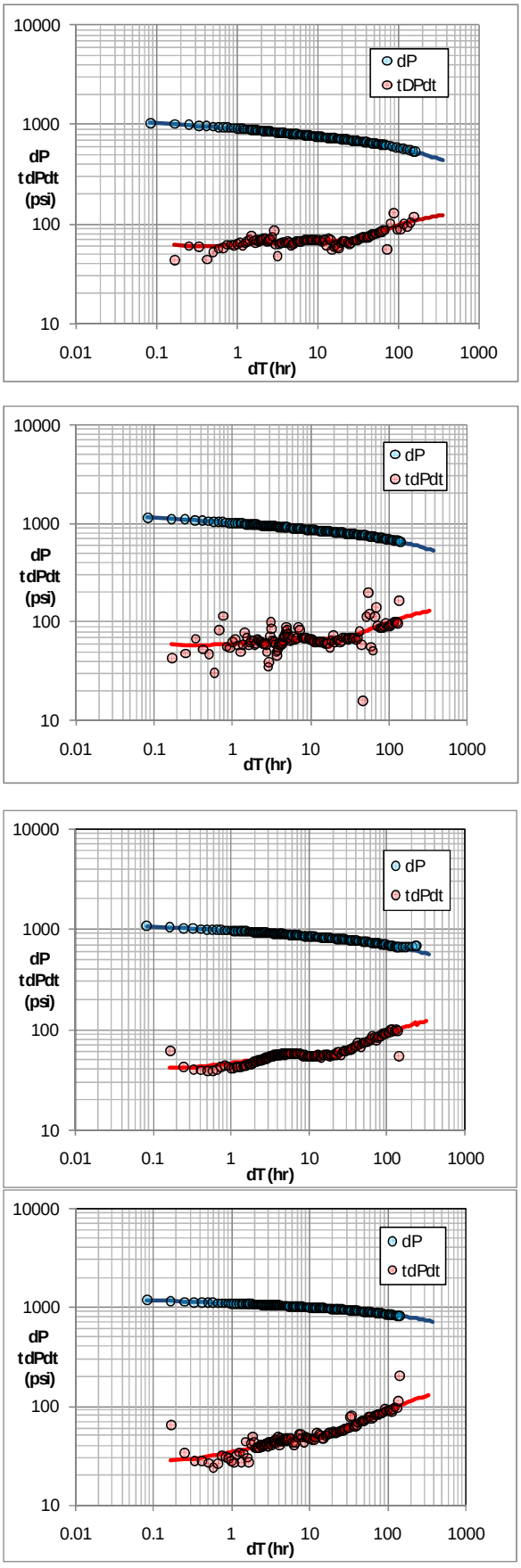

Figure 4. Pressure and pressure derivative match for the 4 PFO tests performed during the injection stimulation. Test 1 is at the top and test 4 at the bottom.

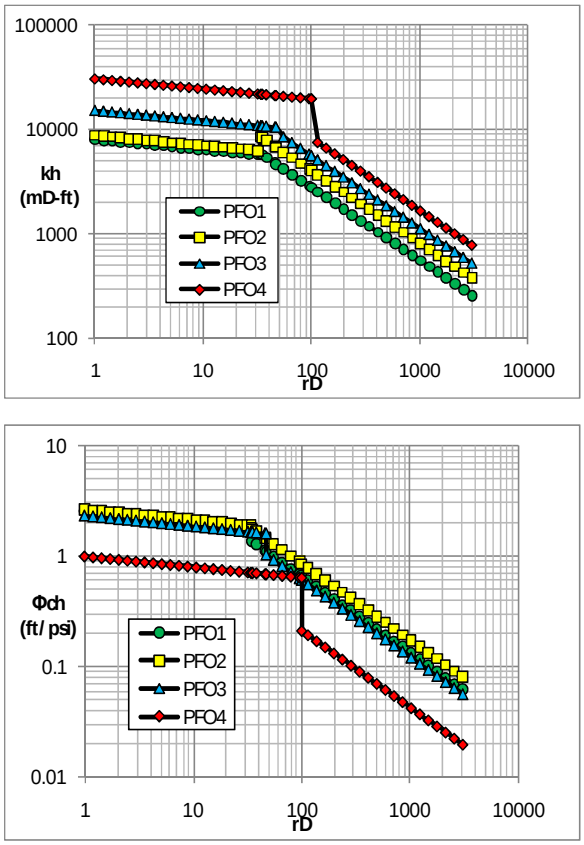

Figure 5. Permeability-thickness (top) and φch (bottom) versus radial distance from the well for all the four PFO tests.

6. CONCLUSIONS

A method for analysis of drawdown and buildups for fractional flow composite reservoirs with low matrix permeability has been presented. For buildups the method relies on the use of diagnostic graphs that is a generalization of the Horner plot for fractional dimensions in each region separately. A relationship was derived to calculate the interface radius when the transition time is known from the derivative plot.

The method seems robust and sensitive and could provide a new way to interpret pressure transient tests in wells where the pressure derivative changes with time.

The method was applied to a sequence of four PFO's for a well under injection stimulation. The results show how the stimulation leads to progressively large permeability as well as extension in size of an inner region of improved conductivity.

The permeability values obtained are consistent with a medium of modest conductivity and their change shows the effectiveness of the stimulation.

Very large values of storativity were obtained which are consequence of dilation in the fracture system. The storativity of the total system increases due to the response of the fracture volume to pressure.

ACKNOWLEDGEMENTS

The permission of Chevron Geothermal and Power to publish this paper is gratefully acknowledged.

REFERENCES

Acuna J.A., Ershaghi I and Yortsos Y.C. Practical Application of Fractal Pressure-Transient Analysis in Naturally Fractured Reservoirs. SPE paper 24705. SPE Formation Evaluation. 1995.

Acuna J.A. Numerical Construction and Fluid Flow Simulation in Networks of Fractures Using Fractal Geometry. PhD Dissertation. University of Southern California. 1993.

Barker J.A. A generalized radial flow model for hydraulic tests in fractured rocks. Water Resources Research 24(10), 1796-1804. 1988.

Chang J. and Yortsos Y.C. Pressure Transient Analysis of Fractal reservoirs. SPE Formation Evaluation 289:311, 1990.

Doe T.W. Fractional Dimension Analysis of Constant-Pressure Well Tests. SPE paper 22702. 1991.

Le Borgne, T., O. Bour, J. R. de Dreuzy, P. Davy, and F. Touchard. Equivalent mean flow models for fractured aquifers: Insights from a pumping tests scaling interpretation, *Water Resour. Res.*, *40*, 2004.

Leveinen J. Composite model with fractional flow dimensions for well test analysis in fractured reservoirs. Journal of Hydrology 234, pp 116-141. 2000.

Palike H. Pumping Tests in Fractal Media. MSc Thesis. University College London. 1998.

Van den Hoek. Pressure Transient Analysis in Fractured Produced Water Injection Wells. SPE paper 77946. 2002.

Yoshioka K., Pasikki R. and Riedel K. Hydraulic Stimulation Techniques Applied to Injection Wells at the Salak Geothermal Field, Indonesia. SPE paper 121184. March 2009.